Electromagnetic field and the chiral magnetic effect in the quark-gluon plasma

Kirill Tuchin

Department of Physics and Astronomy, Iowa State University, Ames, Iowa 50011, USA

Time evolution of an electromagnetic field created in heavy-ion collisions strongly depends on the electromagnetic response of the quark-gluon plasma, which can be described by the Ohmic and chiral conductivities. The latter is intimately related to the chiral magnetic effect. I argue that a solution to the classical Maxwell equations at finite chiral conductivity is unstable due to the soft modes $k < \sigma_\chi$ that grow exponentially with time. In the kinematical region relevant for the relativistic heavy-ion collisions, I derive analytical expressions for the magnetic field of a point charge. I show that finite chiral conductivity causes oscillations of magnetic field at early times.

I. INTRODUCTION

Collision of relativistic heavy ions produces hot nuclear matter that can be described using the relativistic hydrodynamics [1,2]. I will refer to this matter as the quark-gluon plasma (QGP), leaving aside the issues of its equilibration and thermalization. Valence electric charges of the colliding ions are not a part of the plasma, as they continue on the incident trajectory along the beam directions with very little deflection [3]. However, they create a strong electromagnetic field (EMF) that influences the plasma behavior [4–9]. Electrically conducting plasma responds by generating induced EMF. The resulting EMF is a solution to a complicated magnetohydrodynamic problem. As a first approximation, one can rely on slow time dependence of the relevant kinetic coefficients on time to decouple the Maxwell equations from the time evolution of the QGP. Analytical solution to these equations shows that the EMF decreases with time much slower than in vacuum and is approximately collision energy independent; rather it depends only on the impact parameter and the electrical conductivity of the QGP [4,10–12]. Numerical simulations that take into account the QGP expansion [13] qualitatively agree with this conclusion.[1]

It has been recently realized that kinetic properties of the QGP reflect the nontrivial topological structure of the QCD. In particular, the QGP responds to the chirality imbalance by generating metastable parity-odd domains. In the presence of external magnetic field such a metastable domain induces a parallel to it electric field, which is known as the chiral magnetic effect (CME) [9,14–17]. Electric current generated by the CME is proportional to the external magnetic field, with the chiral conductivity σ_χ being the proportionality coefficient. In this paper, I study the electromagnetic field generated by valence charges at finite chiral conductivity and determine the role of the chiral magnetic effect (CME) in the electromagnetic field dynamics in the QGP.

I found a twofold effect of the CME on the electromagnetic field evolution. First, the field becomes unstable because

soft modes with $k < \sigma_\chi$ grow exponentially with time. For the QGP this effect is of little importance since the largest wavelength $1/k$ that is allowed in QGP is much smaller than $1/\sigma_\chi$. However, in non-Abelian plasmas with large spatial extent this is an important phenomenon that may lead to a breakdown of the electromagnetic field into a set of knots with nontrivial topology.[2] Second, due to finite chiral conductivity, the magnetic field, produced by valence electric charges, oscillates at early times after a heavy-ion collision. These oscillations may result in partial cancellation of the magnetic field effects, when averaged over time.

The paper is structured as follows. In Sec. II, I describe the Maxwell-Chern-Simons (MCS) theory, which is an elegant way to incorporate the topological effects in QED. In the MCS the chiral conductivity arises from the time-dependent θ angle. Following Ref. [24] I consider the simplest model with constant σ_χ. In Sec. III, I solve MCS equations away from charges and show that the dispersion relation of electromagnetic wave contains an unstable mode at $k < \sigma_\chi$. In Sec. IV, I derive expressions for the electromagnetic field of a relativistic point charge and discuss its properties. Explicit analytical expressions for the magnetic field of a point charge is derived in Sec. V in the diffusion approximation, which is appropriate for the relativistic heavy-ion collisions. The main result, shown in Fig. 2, indicates that at finite chiral conductivity, magnetic field components oscillate at early times. I discuss these results and conclude in Sec. VI.

II. MAXWELL-CHERN-SIMONS EQUATIONS

The Lagrangian of electrodynamics coupled to the topological charge carried by the gluon field, the so-called Maxwell-Chern-Simons theory, reads [17,25–27]

$$L = -\frac{1}{4}F^{\mu\nu}F_{\mu\nu} - A_\mu j^\mu - \frac{c}{4}\theta \tilde{F}^{\mu\nu}F_{\mu\nu}, \qquad (1)$$

where $c = N_c \sum_f q_f^2 e^2 / 2\pi^2$. An external pseudoscalar field θ depends on the medium properties and originates in the QCD

Lagrangian. The corresponding field equations are given by[3]

$$\nabla \cdot \boldsymbol{B} = 0, \tag{2}$$

$$\nabla \cdot \boldsymbol{E} = \rho - c\,\nabla\theta \cdot \boldsymbol{B}, \tag{3}$$

$$\nabla \times \boldsymbol{E} = -\partial_t \boldsymbol{B}, \tag{4}$$

$$\nabla \times \boldsymbol{B} = \partial_t \boldsymbol{E} + \boldsymbol{j} + c(\partial_t \theta \, \boldsymbol{B} + \nabla\theta \times \boldsymbol{E}). \tag{5}$$

Time-derivative $\dot{\theta} = \mu_5$ can be identified with the axial chemical potential μ_5 [16,17]. The part of the anomalous current density proportional to the magnetic field can be written down as $\boldsymbol{j} = \sigma_\chi \boldsymbol{B}$, where

$$\sigma_\chi = \mu_5 \frac{e^2}{2\pi^2} N_c \sum_f q_f^2 \tag{6}$$

is the chiral conductivity induced by the QED anomaly [29]. The θ angle is believed to be finite inside metastable regions of size $\sim 1/g^2 T$. On average it must vanish $\langle\theta\rangle = 0$ to preserve the global $\mathcal{CP}$ invariance of the QCD. Its space and time dynamics is complicated: shortly after a heavy-ion collision it is determined by the colored fields of glasma [30–32], while at later time by the sphaleron transition dynamics [20–23].

Since the detailed structure of inhomogeneous field θ is unknown, one has to resort to phenomenological models in order to study its effect on the electromagnetic field dynamics (see, e.g., Ref. [32]). The simplest model that captures the essential dynamics of the CME effect, and that we adopt in the present study, is to neglect the space variation of θ and approximate σ_χ by a constant. In other words we set $\nabla\theta = 0$ and $\sigma_\chi = \text{const}$. This model was used in Ref. [33] to discuss nontrivial static topological solutions of (2)–(5) (see below) and in Ref. [24] to numerically investigate time evolution of magnetic field. The main advantage of this model is that it can be analytically solved and thus provides important insights into the dynamics of the electromagnetic fields in the presence of the chiral anomaly. Moreover, it is argued in Refs. [34,35] that θ may actually be a slow function of x that permits expansion $\theta \approx \theta_0 + \mu_5 t + c^{-1}\boldsymbol{P} \cdot \boldsymbol{r}$ with constant μ_5 and $\boldsymbol{P}$.

Consider now the system of equations (2)–(5) in the absence of electric charges, with the assumptions discussed in the previous paragraph. It has nontrivial stationary solutions with finite magnetic field and vanishing electric field that satisfies the following equations [36–38]:

$$\nabla \cdot \boldsymbol{B} = 0, \tag{7}$$

$$\nabla \times \boldsymbol{B} = \sigma_\chi \boldsymbol{B}. \tag{8}$$

It is argued in Ref. [33] that since the anomalous current $\boldsymbol{j} = \sigma_\chi \boldsymbol{B}$ exists only in the deconfined phase occupying a domain of finite volume D, there is no outward current on its boundary. This implies the boundary condition

$$\hat{\boldsymbol{r}} \cdot \boldsymbol{B}|_{\partial D} = 0. \tag{9}$$

The solution to (7)–(9) is a system of magnetized knots of different sizes. In a simplest case of spherical boundary the

possible values of its radius are

$$R_n = \frac{\kappa_n}{\sigma_\chi}, \quad n = 0, 1, 2, \ldots, \tag{10}$$

where n enumerates zeros of spherical Bessel functions κ_n. The smallest of κ's is $\kappa_0 \approx 4.5$, which for a realistic σ_χ yields $R_0 \approx 200$ fm. R_0 is much larger than a characteristic transverse size of the QGP $R_A \sim 6$–10 fm and thus has no effect on the QGP phenomenology. It is possible that magnetic knots are artifacts of our model for the θ angle. It is far from clear whether any static topological solutions survive in a more realistic model.

III. INSTABILITY OF ELECTROMAGNETIC WAVES IN INFINITE PLASMA

Consider electromagnetic waves propagating in plasma far from any sources. In a conducting medium Maxwell equations for the electromagnetic field read

$$\nabla \cdot \boldsymbol{B} = 0, \tag{11}$$

$$\nabla \cdot \boldsymbol{D} = 0, \tag{12}$$

$$\nabla \times \boldsymbol{E} = -\partial_t \boldsymbol{B}, \tag{13}$$

$$\nabla \times \boldsymbol{H} = \partial_t \boldsymbol{D} + \sigma_\chi \boldsymbol{B}. \tag{14}$$

$\boldsymbol{D}$ is electric displacement vector. We will assume that $\mu = 1$. Fourier transformation

$$\boldsymbol{E}(\boldsymbol{r}, t) = \int \frac{d^4 k}{(2\pi)^4} e^{-ik \cdot x} \boldsymbol{E}_{\omega, \boldsymbol{k}},$$
$$\boldsymbol{B}(\boldsymbol{r}, t) = \int \frac{d^4 k}{(2\pi)^4} e^{-ik \cdot x} \boldsymbol{B}_{\omega, \boldsymbol{k}}, \tag{15}$$

where $x = (t, \boldsymbol{r})$, $k = (\omega, \boldsymbol{k})$ yields Maxwell equations in momentum space

$$\boldsymbol{k} \cdot \boldsymbol{B}_{\omega, \boldsymbol{k}} = 0, \tag{16}$$

$$\epsilon \boldsymbol{k} \cdot \boldsymbol{E}_{\omega, \boldsymbol{k}} = 0, \tag{17}$$

$$\boldsymbol{k} \times \boldsymbol{E}_{\omega, \boldsymbol{k}} = \omega \boldsymbol{B}_{\omega, \boldsymbol{k}}, \tag{18}$$

$$\boldsymbol{k} \times \boldsymbol{B}_{\omega, \boldsymbol{k}} = -\omega \epsilon \boldsymbol{E}_{\omega, \boldsymbol{k}} - i\sigma_\chi \boldsymbol{B}_{\omega, \boldsymbol{k}}, \tag{19}$$

where $\boldsymbol{D}_{\omega, \boldsymbol{k}} = \epsilon \boldsymbol{E}_{\omega, \boldsymbol{k}}$. In electrically conducting medium with the Ohmic conductivity σ the permittivity is $\epsilon = 1 + i\sigma/\omega$, Taking vector product of (19) with $\boldsymbol{k}$ and using (16) and (18) we get

$$\boldsymbol{B}_{\omega, \boldsymbol{k}}[\omega(\omega + i\sigma) - k^2] = -i\sigma_\chi \boldsymbol{k} \times \boldsymbol{B}_{\omega, \boldsymbol{k}}. \tag{20}$$

Taking another vector product with $\boldsymbol{k}$ gives

$$(\boldsymbol{k} \times \boldsymbol{B}_{\omega, \boldsymbol{k}})[\omega(\omega + i\sigma) - k^2] = i\sigma_\chi k^2 \boldsymbol{B}_{\omega, \boldsymbol{k}}. \tag{21}$$

Equations (20) and (21) have a nontrivial solution only if the following dispersion relation is satisfied

$$[\omega(\omega + i\sigma) - k^2]^2 = \sigma_\chi^2 k^2. \tag{22}$$

It has four solutions

$$\omega_{\lambda_1, \lambda_2} = -\frac{i\sigma}{2} + \lambda_1 \sqrt{k^2 + \lambda_2 \sigma_\chi k - \sigma^2/4}, \tag{23}$$

---

[3]The correct signs in front of the anomalous terms where derived in Ref. [28].

where $\lambda_1, \lambda_2 = \pm 1$ and $k = \sqrt{\boldsymbol{k}^2} \geqslant 0$. These solutions determine the time dependence of electromagnetic wave as $\sim e^{-i\omega_{\lambda_1,\lambda_2}t}$.

Let $\kappa^2 = k^2 + \lambda_2 \sigma_\chi k - \sigma^2/4$. When $\kappa^2 > 0$ the electromagnetic wave oscillates with frequency κ and is damped over the distance $1/\sigma$. This corresponds to momenta

$$k > k_0 \equiv \frac{1}{2}\sqrt{\sigma_\chi^2 + \sigma^2} - \frac{\lambda_2 \sigma_\chi}{2}. \qquad (24)$$

For $k < k_0$, $\kappa^2 < 0$, and all $\omega_{\lambda_1,\lambda_2}$'s become imaginary implying that electromagnetic wave is a monotonic function of time. At $\kappa^2 = -\sigma^2/4$, which occurs at $k = \sigma_\chi$, $\lambda_2 = -1$, and $\lambda_1 = +1$, ω_{+-} vanishes indicating a stationary mode. Finally, when $\kappa^2 < -\sigma^2/4$, i.e., $k < \sigma_\chi$, $\lambda_2 = -1$, $\lambda_1 = +1$ there is an unstable mode with Im $\omega_{+-} > 0$, which corresponds to the exponentially increasing magnetic field. Im ω_{+-} vanishes at $k = 0$ and $k = \sigma_\chi$ and has a maximum value of $(\sqrt{\sigma^2 + \sigma_\chi^2} - \sigma)/2$ at $k = \sigma_\chi/2$.

The electromagnetic wave, which at some initial time contains modes extending to the region $k < \sigma_\chi$, is unstable. This is a usual situation in an infinite plasma. However, in a plasma of spatial size R there are only modes $k \gtrsim 1/R$. Therefore, the instability affects the field evolution only if $R \gtrsim 1/\sigma_\chi$. In the QGP this condition is not satisfied, except, perhaps, in very rare fluctuations of the θ angle, and hence can be ignored.

IV. ELECTROMAGNETIC FIELD OF A POINT CHARGE

In an electrically conducting medium Maxwell equations for the electromagnetic field of a point charge moving along a straight line $z = vt$ read

$$\nabla \cdot \boldsymbol{B} = 0, \qquad (25)$$

$$\nabla \cdot \boldsymbol{D} = e\delta(z - vt)\delta(\boldsymbol{b}), \qquad (26)$$

$$\nabla \times \boldsymbol{E} = -\partial_t \boldsymbol{B}, \qquad (27)$$

$$\nabla \times \boldsymbol{H} = \partial_t \boldsymbol{D} + \sigma_\chi \boldsymbol{B} + ev\hat{\boldsymbol{z}}\delta(z - vt)\delta(\boldsymbol{b}). \qquad (28)$$

These equations in momentum space are

$$\boldsymbol{k} \cdot \boldsymbol{B}_{\omega,\boldsymbol{k}} = 0, \qquad (29)$$

$$\epsilon \boldsymbol{k} \cdot \boldsymbol{E}_{\omega,\boldsymbol{k}} = -2\pi i e \delta(\omega - k_z v), \qquad (30)$$

$$\boldsymbol{k} \times \boldsymbol{E}_{\omega,\boldsymbol{k}} = \omega \boldsymbol{B}_{\omega,\boldsymbol{k}}, \qquad (31)$$

$$\boldsymbol{k} \times \boldsymbol{B}_{\omega,\boldsymbol{k}} = -\omega\epsilon \boldsymbol{E}_{\omega,\boldsymbol{k}} - i\sigma_\chi \boldsymbol{B}_{\omega,\boldsymbol{k}} - 2\pi i e v\hat{\boldsymbol{z}}\delta(\omega - k_z v). \qquad (32)$$

We repeat the algebraic manipulations of the previous section. First, taking the vector product of (32) with $\boldsymbol{k}$ and using (29) and (31) we arrive at

$$\boldsymbol{B}_{\omega,\boldsymbol{k}}[\omega(\omega + i\sigma) - k^2]$$
$$= -i\sigma_\chi \boldsymbol{k} \times \boldsymbol{B}_{\omega,\boldsymbol{k}} - 2\pi i e v\boldsymbol{k} \times \hat{\boldsymbol{z}}\delta(\omega - k_z v). \qquad (33)$$

Second, we take another vector product with $\boldsymbol{k}$ to obtain

$$(\boldsymbol{k} \times \boldsymbol{B}_{\omega,\boldsymbol{k}})[\omega(\omega + i\sigma) - k^2]$$
$$= i\sigma_\chi k^2 \boldsymbol{B}_{\omega,\boldsymbol{k}} - 2\pi i e v\boldsymbol{k} \times (\boldsymbol{k} \times \hat{\boldsymbol{z}})\delta(\omega - k_z v). \qquad (34)$$

We are interested in a particular solution to Eqs. (33) and (34), namely the one that is generated by the electric charge e. Solving (33) and (34) yields

$$\boldsymbol{B}_{\omega,\boldsymbol{k}} = \frac{(\boldsymbol{k} \times \hat{\boldsymbol{z}})[\omega(\omega + i\sigma) - k^2] - i\sigma_\chi \boldsymbol{k} \times (\boldsymbol{k} \times \hat{\boldsymbol{z}})}{[\omega(\omega + i\sigma) - k^2]^2 - \sigma_\chi^2 k^2}$$
$$\times (-2\pi i)ev\delta(\omega - k_z v). \qquad (35)$$

The electric field follows from the Faraday law (31) upon taking its vector product with $\boldsymbol{k}$:

$$\boldsymbol{k}(\boldsymbol{k} \cdot \boldsymbol{E}_{\omega,\boldsymbol{k}}) - k^2 \boldsymbol{E}_{\omega,\boldsymbol{k}} = \omega(\boldsymbol{k} \times \boldsymbol{B}_{\omega,\boldsymbol{k}}). \qquad (36)$$

Substituting (30) and (32) we find

$$\boldsymbol{E}_{\omega,\boldsymbol{k}} = \frac{2\pi i e \delta(\omega - k_z v)[\boldsymbol{k}/\epsilon - v\omega\hat{\boldsymbol{z}}] - i\omega\sigma_\chi \boldsymbol{B}_{\omega,\boldsymbol{k}}}{\omega(\omega + i\sigma) - k^2}, \qquad (37)$$

with $\boldsymbol{B}_{\omega,\boldsymbol{k}}$ given by (35).

It will be suitable to write the cross products in Eq. (35) in cylindrical coordinates. Let ψ be the angle between the vector $\boldsymbol{k}_\perp$ and the x axis, the corresponding unit vector is $\hat{\boldsymbol{\psi}} = -\hat{\boldsymbol{x}} \sin \psi + \hat{\boldsymbol{y}} \cos \psi$. Then

$$\boldsymbol{k} \times \hat{\boldsymbol{z}} = -k_\perp \hat{\boldsymbol{\psi}}, \qquad (38)$$

$$\boldsymbol{k} \times (\boldsymbol{k} \times \hat{\boldsymbol{z}}) = k_z \boldsymbol{k}_\perp - k_\perp^2 \hat{\boldsymbol{z}}. \qquad (39)$$

Using identities (38) and (39) in Eq. (30), substituting the result into (15), and taking integral over k_z we find

$$\boldsymbol{B} = ie \int_{-\infty}^{+\infty} \frac{d\omega}{2\pi} \int \frac{d^2 k_\perp}{(2\pi)^2} \frac{k_\perp \hat{\boldsymbol{\psi}}\left[\omega(\omega + i\sigma) - k_\perp^2 - \frac{\omega^2}{v^2}\right] + i\sigma_\chi\left(\boldsymbol{k}_\perp \frac{\omega}{v} - k_\perp^2 \hat{\boldsymbol{z}}\right)}{\left[\omega(\omega + i\sigma) - k_\perp^2 - \frac{\omega^2}{v^2}\right]^2 - \sigma_\chi^2\left(k_\perp^2 + \frac{\omega^2}{v^2}\right)} e^{-i\omega x_- + i\boldsymbol{k}_\perp \cdot \boldsymbol{b}}, \qquad (40)$$

where $x_- = t - z/v$.

The time dependence of the magnetic field is determined by the poles of (35) in the plane of complex ω. These poles are solutions of the following quartic equation

$$\left[\omega(\omega + i\sigma) - k_\perp^2 - \frac{\omega^2}{v^2}\right]^2 - \sigma_\chi^2\left(k_\perp^2 + \frac{\omega^2}{v^2}\right) = 0. \qquad (41)$$

Equation (41) can be obtained from the dispersion relation (22) of a free wave by restricting it to the particle equation of

motion $k_z = \omega/v$. Introducing $\gamma = (1 - v^2)^{-1/2}$ allows us to cast (41) in a more convenient form

$$\left(-\frac{\omega^2}{v^2\gamma^2} + i\omega\sigma - k_\perp^2\right)^2 - \sigma_\chi^2\left(\frac{\omega^2}{v^2} + k_\perp^2\right) = 0. \qquad (42)$$

Four solutions to this equation can be found using the standard algebraic methods. However, they are quite bulky, so I am not reproducing them here. Instead, I find it more illuminating to
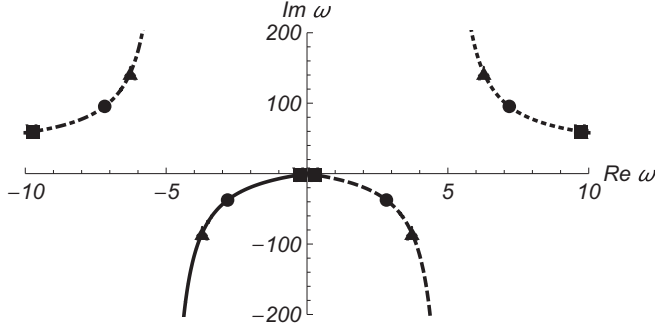
FIG. 1. Four solutions of (42) at $\sigma = 5.8$ MeV, $\sigma_\chi = 1$ MeV, $\gamma = 100$. Horizontal and vertical axes are in units of GeV. Each line is a unique function of $k_\perp$. Squares, circles and triangles indicate the positions of the poles at $k_\perp = 0.1, 0.6, 1.1$ GeV respectively.

plot them at fixed σ, σ_χ, and γ for different values of $k_\perp$ as shown in Fig. 1.

The position of the four poles at $k_\perp \to 0$ can be found by expanding (42), which gives three distinct solutions $\omega = 0$ and $\omega = v^2\gamma^2(i\sigma \pm \sigma_\chi)$. The former corresponds to the minimum value of the lower branches, while the latter to the minimum values of the upper branches. Thus, the upper branches are separated from the real axis by a gap $v^2\gamma^2\sigma$. The absolute value of the real part of the upper branches decreases monotonically with $k_\perp$. At $k_\perp \to \infty$

$$\omega \approx \pm i v\gamma k_\perp \pm \tfrac{1}{2} v\gamma \sigma_\chi \sqrt{\gamma^2 - 1}. \qquad (43)$$

Thus, the real value of ω of upper branches approaches a constant at large $k_\perp$, which indicates that a gap of size $\sim \gamma^2 \sigma_\chi$ exists also between the upper branches and the imaginary axis. In the ultrarelativistic limit $v \to 1$, or $\gamma \to \infty$, the upper branches move to infinity. Since the poles in the upper half plane determine the electromagnetic field at $x_- < 0$, it gets exponentially suppressed at $\gamma \gg 1$.

Behavior of the electromagnetic field at $x_- > 0$ is determined by the two poles in the lower half plane. Unlike the poles in the upper half plane they stay finite in the ultrarelativistic limit. One of the lower branches exhibits a peculiar behavior by crossing the real axis and acquiring a positive $\text{Im}\,\omega$ when $k_\perp < \sigma_\chi$. This is a way in which the field instability discussed in the previous section manifests itself in this case. (This feature is not readily seen in Fig. 1 due to the small value of σ_χ.) The existence of a pole in the upper-half plane implies that the field of a point charge moving along $x_- = 0$ receives acausal contribution, viz., a term that is finite at $x_- < 0$ when $\gamma \to \infty$. Fortunately, transverse momenta as small as $k_\perp \sim \sigma_\chi$ are not relevant in relativistic heavy-ion phenomenology, allowing me to neglect the acausal contribution. This however does not resolve a theoretical problem that the acausal term presents.[4]

---

[4]A solution to this problem might be related to existence magnetic knots discussed in Sec. II that also appear at $k \sim \sigma_\chi$.

V. DIFFUSION APPROXIMATION

At a given light-cone time $x_- > 0$ the ω integral in Eq. (40) vanishes at $\omega \gg 1/x_-$ due to the rapid oscillation of the integrand. Therefore, at later times the terms in Eq. (42) that are quadratic in ω are suppressed. This correspond to the following diffusion approximation:

$$\omega \ll \sigma v^2\gamma^2, \quad \omega \ll v\gamma k_\perp, \qquad (44)$$

which is tantamount to

$$x_- \gg \frac{1}{\sigma v^2\gamma^2}, \quad x_- \gg \frac{b}{v\gamma}, \qquad (45)$$

where we estimated $k_\perp \sim 1/b$. Electrical conductivity of the quark-gluon plasma at the critical temperature is $\sigma = 5.8$ MeV [39–42]. For a heavy-ion collision at $\gamma = 100$ we estimate $1/\sigma v^2\gamma^2 \sim 3 \times 10^{-3}$ fm. For $b \sim 10$ fm, $b/\gamma \sim 0.1$ fm. Taking into account that it takes about $1/Q_s \sim 0.2$ fm to release the color charges from the nuclei wave functions, it follows that approximation (44) applies to the entire lifetime of the QGP. The precise initial conditions do not play an important role in the electromagnetic field evolution.

Since the valence quarks are ultrarelativistic, i.e., $\gamma \gg 1$, we will approximate their velocity as $v \approx 1 - 1/2\gamma^2$. Then, the dispersion relation (42) in the diffusion approximation takes form

$$(i\omega\sigma - k_\perp^2)^2 - \sigma_\chi^2(\omega^2 + k_\perp^2) = 0. \qquad (46)$$

The two solutions of (46), describing the two lower poles in Fig. 1, are

$$\omega_{1,2} = \frac{-i\sigma k_\perp^2 \pm k_\perp \sigma_\chi \sqrt{k_\perp^2 - \sigma^2 - \sigma_\chi^2}}{\sigma^2 + \sigma_\chi^2}. \qquad (47)$$

These are the only poles of the Fourier component of magnetic field $\boldsymbol{B}_{\omega,\boldsymbol{k}}$ in the complex ω plane because the upper poles in Fig. 1 disappear in the limit $v \to 1$. If $k_\perp > \sqrt{\sigma^2 + \sigma_\chi^2}$, then both complex-conjugated poles lie in the lower half plane. If $\sigma_\chi < k_\perp < \sqrt{\sigma^2 + \sigma_\chi^2}$, then there are two poles on the imaginary axis in the lower half plane. Finally, if $k_\perp < \sigma_\chi$, then both poles lie on the imaginary axis, but ω_1 is in the upper half plane, while ω_2 is still in the lower one.

In the diffusion approximation (40) reads

$$\boldsymbol{B} = -ie \int \frac{d\omega}{2\pi} \int \frac{d^2k_\perp}{(2\pi)^2} \frac{k_\perp \hat{\boldsymbol{\psi}}(i\omega\sigma - k_\perp^2) + i\sigma_\chi(\boldsymbol{k}_\perp\omega - k_\perp^2 \hat{\boldsymbol{z}})}{(\sigma^2 + \sigma_\chi^2)(\omega - \omega_1)(\omega - \omega_2)}$$
$$\times e^{-i\omega x_- + i\boldsymbol{k}_\perp \cdot \boldsymbol{b}} \qquad (48)$$

$$= \int \frac{d^2k_\perp}{(2\pi)^2} e^{i\boldsymbol{k}_\perp \cdot \boldsymbol{b}} \int_{-\infty}^{+\infty} \frac{d\omega}{2\pi} \frac{\boldsymbol{f}(\omega)}{(\omega - \omega_1)(\omega - \omega_2)} e^{-i\omega x_-}, \quad (49)$$

where I denoted

$$\boldsymbol{f}(\omega) = -\frac{ie}{\sigma^2 + \sigma_\chi^2}[k_\perp \hat{\boldsymbol{\psi}}(i\omega\sigma - k_\perp^2) + i\sigma_\chi(\boldsymbol{k}_\perp\omega - k_\perp^2 \hat{\boldsymbol{z}})].$$
$$(50)$$

Closing the integration contour in Eq. (49) by an infinite semicircle in the lower half plane we find at $x_- > 0$

$$\boldsymbol{B} = \int \frac{d^2 k_\perp}{(2\pi)^2} e^{i\boldsymbol{k}_\perp \cdot \boldsymbol{b}} \frac{i}{\omega_2 - \omega_1}$$
$$\times [e^{-i\omega_1 x_-} \boldsymbol{f}(\omega_1)\theta(k_\perp - \sigma_\chi) - e^{-i\omega_2 x_-} \boldsymbol{f}(\omega_2)]\theta(x_-). \tag{51}$$

The value of σ_χ probably does not exceed a few MeV at best, while typical $k_\perp$ is in the range 20–200 MeV corresponding to b's in the range 1–10 fm. Therefore, only the case $k_\perp^2 \gg \sigma^2 + \sigma_\chi^2$ has a practical significance. This allows us to approximate the poles of (47) as follows

$$\omega_{1,2} \approx \frac{k_\perp^2(-i\sigma \pm \sigma_\chi)}{\sigma^2 + \sigma_\chi^2} = \frac{k_\perp^2}{i\sigma \pm \sigma_\chi}. \tag{52}$$

The magnetic field at $x_- > 0$ becomes

$$\boldsymbol{B} \approx \int \frac{d^2 k_\perp}{(2\pi)^2} e^{i\boldsymbol{k}_\perp \cdot \boldsymbol{b}} \frac{i}{\omega_2 - \omega_1}[e^{-i\omega_1 x_-} \boldsymbol{f}(\omega_1) - e^{-i\omega_2 x_-} \boldsymbol{f}(\omega_2)]. \tag{53}$$

Its polar component is given by

$$B_\phi = \int \frac{d^2 k_\perp}{(2\pi)^2} e^{i\boldsymbol{k}_\perp \cdot \boldsymbol{b}} \frac{i}{\omega_2 - \omega_1} \hat{\boldsymbol{\psi}} \cdot [e^{-i\omega_1 x_-} \boldsymbol{f}(\omega_1)$$
$$- e^{-i\omega_2 x_-} \boldsymbol{f}(\omega_2)], \tag{54}$$

where ϕ is the angle between the impact parameter $\boldsymbol{b}$ and the x axis. Integration over the directions of $\boldsymbol{k}_\perp$ given by the polar angle ψ is done as follows:

$$\int_0^{2\pi} e^{i\boldsymbol{k}_\perp \cdot \boldsymbol{b}} \hat{\boldsymbol{\psi}}\, d\psi = \int_0^{2\pi} e^{ik_\perp b \cos(\psi - \phi)} (-\hat{\boldsymbol{x}} \sin \psi + \hat{\boldsymbol{y}} \cos \psi) d\psi$$
$$= 2\pi i J_1(k_\perp b)\hat{\boldsymbol{\phi}}, \tag{55}$$

Using (55) in Eq. (54) and substituting (50) and (52) we have:

$$B_\phi = -\int_0^\infty \frac{dk_\perp k_\perp}{2\pi} i J_1(k_\perp b) \frac{ek_\perp}{2(\sigma^2 + \sigma_\chi^2)}$$
$$\times \left[(i\sigma - \sigma_\chi)e^{-i\frac{k_\perp^2 x_-}{i\sigma + \sigma_\chi}} + (i\sigma + \sigma_\chi)e^{-i\frac{k_\perp^2 x_-}{i\sigma - \sigma_\chi}} \right]. \tag{56}$$

The remaining integral can be done analytically yielding

$$B_\phi = \frac{eb}{8\pi x_-^2} e^{-\frac{b^2 \sigma}{4x_-}} \left[\sigma \cos\left(\frac{b^2 \sigma_\chi}{4x_-}\right) + \sigma_\chi \sin\left(\frac{b^2 \sigma_\chi}{4x_-}\right) \right]. \tag{57}$$

Turning to the component of magnetic field aligned along the $\boldsymbol{b}$ direction we obtain:

$$B_r = \int \frac{d^2 k_\perp}{(2\pi)^2} e^{i\boldsymbol{k}_\perp \cdot \boldsymbol{b}} \frac{i}{\omega_2 - \omega_1} \hat{\boldsymbol{k}}_\perp \cdot$$
$$\times [e^{-i\omega_1 x_-} \boldsymbol{f}(\omega_1) - e^{-i\omega_2 x_-} \boldsymbol{f}(\omega_2)]. \tag{58}$$

Angular integration is done using

$$\int_0^{2\pi} e^{i\boldsymbol{k}_\perp \cdot \boldsymbol{b}} \hat{\boldsymbol{k}}_\perp\, d\psi = \int_0^{2\pi} e^{ik_\perp b \cos(\psi - \phi)} (\hat{\boldsymbol{x}} \cos \psi + \hat{\boldsymbol{y}} \sin \psi) d\psi$$
$$= 2\pi i J_1(k_\perp b)\hat{\boldsymbol{b}}. \tag{59}$$

Plugging the $k_\perp$ component of $\boldsymbol{f}$ from (50) and integrating over $k_\perp$ we derive

$$B_r = \frac{eb}{8\pi x_-^2} e^{-\frac{b^2 \sigma}{4x_-}} \left[\sigma \sin\left(\frac{b^2 \sigma_\chi}{4x_-}\right) - \sigma_\chi \cos\left(\frac{b^2 \sigma_\chi}{4x_-}\right) \right]. \tag{60}$$

Finally, repeating the by now familiar procedure and using the integral

$$\int_0^{2\pi} e^{i\boldsymbol{k}_\perp \cdot \boldsymbol{b}} \hat{\boldsymbol{z}}\, d\psi = 2\pi J_0(k_\perp b)\hat{\boldsymbol{z}} \tag{61}$$

we find for the longitudinal field component:

$$B_z = \frac{eb}{4\pi x_-^2} e^{-\frac{b^2 \sigma}{4x_-}} \left[\sigma \sin\left(\frac{b^2 \sigma_\chi}{4x_-}\right) - \sigma_\chi \cos\left(\frac{b^2 \sigma_\chi}{4x_-}\right) \right]. \tag{62}$$
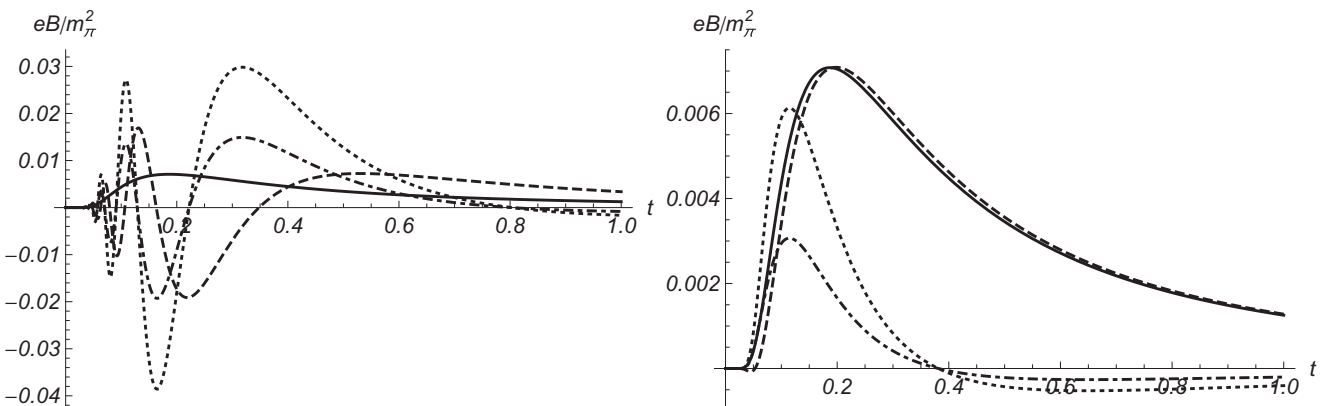

FIG. 2. Magnetic field of a point charge as a function of time t at $z = 0$. (Free space contribution is not shown). Electrical conductivity $\sigma = 5.8$ MeV. Solid line on both panels corresponds to $B = B_\phi$ at $\sigma_\chi = 0$. Broken lines correspond to B_ϕ (dashed), B_r (dashed-dotted), and B_z (dotted) with $\sigma_\chi = 15$ MeV on the left panel and $\sigma_\chi = 1.5$ MeV on the right panel. Note that the vertical scale on the two panels is different.

It is seen in Eqs. (60) and (62) that the field components B_r and B_z are generated only at a finite chiral conductivity σ_χ.

Equations (57), (58), and (62) are the main result of this paper. They show that at finite σ_χ, the magnetic field of a point charge acquires two components that are absent in the chirally neutral medium: the radial and the longitudinal components. All field components oscillate at early times. This is clearly seen in Fig. 2. The B_z and B_r components change sign at light-cone times

$$x_-^{(n)} = \frac{b^2 \sigma_\chi}{4\left[\arctan \frac{\sigma_\chi}{\sigma} + \pi n\right]}, \quad n = 0, 1, \ldots, \quad (63)$$

while the B_ϕ components change sign at

$$\tilde{x}_-^{(n)} = \frac{b^2 \sigma_\chi}{4\left[-\arctan \frac{\sigma}{\sigma_\chi} + \pi n\right]}, \quad n = 0, 1, \ldots. \quad (64)$$

The latest oscillation corresponds to $n = 0$; it increases with σ_χ.

VI. DISCUSSION AND SUMMARY

We discussed the chiral topological effect on the electromagnetic field in the quark-gluon plasma. In our model the anomalous current density is given by $\boldsymbol{j} = \sigma_\chi \boldsymbol{B}$ with constant chiral conductivity σ_χ. For the energy and time scales of the QGP this model gives a reasonable physical picture of the electromagnetic field space-time evolution. There are two major results presented in this paper.

(i) I showed that solutions to the Maxwell equations are not stable in the presence of the chirality imbalance. It is possible that electromagnetic field collapses into a set of magnetic knots. This problem certainly deserves a dedicated study and may be important in cosmology. However, as far as heavy-ion collisions are concerned, this instability has negligible impact on the QGP because it originates from soft modes $k < \sigma_\chi$ that do not exist in the QGP of realistic dimensions. The maximal growth rate of unstable modes is $(\sqrt{\sigma^2 + \sigma_\chi^2} - \sigma)/2$.

(ii) I derived an analytical expression for the magnetic field produced by valence charges in quark-gluon plasma at finite chiral conductivity σ_χ. Its components are given by Eqs. (57), (60), and (62), which indicate the emergence of the radial B_r and longitudinal B_z components of magnetic field (as compared to the $\sigma_\chi = 0$ case). If σ_χ is not much smaller than σ, then all components perform oscillations at early times after the collision. Since the magnetic field is strongest at early times, these oscillations should have important impact on heavy-ion phenomenology. In particular, they may weaken effects that depend on the magnetic field direction, such as the B-dependent elliptic flow [43,44] and charge separation effect [9]. This is especially true for the charge separation effect that requires sufficiently large σ_χ.

In this paper, I considered the simplest model that incorporates the chiral anomaly in electrodynamics. Its main advantages are that it describes the experimentally observable charge separation in heavy-ion collisions and can be solved analytically. However, it has serious drawbacks as well: chiral conductivity of a realistic plasma is a complicated function of space and time. Thus, the main outstanding problem is to find a more realistic model for the chiral anomaly and verify which of the above results survive in an improved formulation, and to what extent. This can serve as a benchmark for the full magnetohydrodynamical treatment of the problem.

[1] L. D. Landau, Izv. Akad. Nauk Ser. Fiz. **17**, 51 (1953).

[2] S. Z. Belenkij and L. D. Landau, Il Nuovo Cim. Suppl. **3S10**, 15 (1956) [Usp. Fiz. Nauk **56**, 309 (1955)].

[3] K. Itakura, Y. V. Kovchegov, L. McLerran, and D. Teaney, Nucl. Phys. A **730**, 160 (2004).

[4] K. Tuchin, Adv. High Energy Phys. **2013**, 490495 (2013).

[5] V. Voronyuk, V. D. Toneev, W. Cassing, E. L. Bratkovskaya, V. P. Konchakovski, and S. A. Voloshin, Phys. Rev. C **83**, 054911 (2011).

[6] V. Skokov, A. Y. Illarionov, and V. Toneev, Int. J. Mod. Phys. A **24**, 5925 (2009).

[7] W.-T. Deng and X.-G. Huang, Phys. Rev. C **85**, 044907 (2012).

[8] A. Bzdak and V. Skokov, Phys. Lett. B **710**, 171 (2012).

[9] D. E. Kharzeev, L. D. McLerran, and H. J. Warringa, Nucl. Phys. A **803**, 227 (2008).

[10] K. Tuchin, Phys. Rev. C **82**, 034904 (2010); **83**, 039903 (2011).

[11] K. Tuchin, Phys. Rev. C **88**, 024911 (2013).

[12] U. Gursoy, D. Kharzeev, and K. Rajagopal, Phys. Rev. C **89**, 054905 (2014).

[13] B. G. Zakharov, Phys. Lett. B **737**, 262 (2014).

[14] D. Kharzeev, Phys. Lett. B **633**, 260 (2006).

[15] D. Kharzeev and A. Zhitnitsky, Nucl. Phys. A **797**, 67 (2007).

[16] K. Fukushima, D. E. Kharzeev, and H. J. Warringa, Phys. Rev. D **78**, 074033 (2008).

[17] D. E. Kharzeev, Ann. Phys. (NY) **325**, 205 (2010).

[18] Y. Akamatsu and N. Yamamoto, Phys. Rev. Lett. **111**, 052002 (2013).

[19] Y. Akamatsu and N. Yamamoto, Phys. Rev. D **90**, 125031 (2014).

[20] M. Joyce and M. E. Shaposhnikov, Phys. Rev. Lett. **79**, 1193 (1997).

[21] A. Boyarsky, J. Frohlich, and O. Ruchayskiy, Phys. Rev. Lett. **108**, 031301 (2012).

[22] H. Tashiro, T. Vachaspati, and A. Vilenkin, Phys. Rev. D **86**, 105033 (2012).

[23] D. Grabowska, D. B. Kaplan, and S. Reddy, Phys. Rev. D **91**, 085035 (2015).

[24] L. McLerran and V. Skokov, Nucl. Phys. A **929**, 184 (2014.)

[25] F. Wilczek, Phys. Rev. Lett. **58**, 1799 (1987).

[26] S. M. Carroll, G. B. Field, and R. Jackiw, Phys. Rev. D **41**, 1231 (1990).

[27] P. Sikivie, Phys. Lett. B **137**, 353 (1984).

[28] S. Ozonder, Phys. Rev. C **81**, 062201 (2010); **84**, 019903 (2011).

[29] D. E. Kharzeev and H. J. Warringa, Phys. Rev. D **80**, 034028 (2009).

[30] D. Kharzeev, A. Krasnitz, and R. Venugopalan, Phys. Lett. B **545**, 298 (2002).

[31] T. Lappi and L. McLerran, Nucl. Phys. A **772**, 200 (2006).

[32] Y. Hirono, T. Hirano, and D. E. Kharzeev, arXiv:1412.0311 [hep-ph].

[33] M. N. Chernodub, arXiv:1002.1473 [nucl-th].

[34] A. R. Zhitnitsky, arXiv:1411.2606 [hep-ph].

[35] A. R. Zhitnitsky, Phys. Rev. D **90**, 105007 (2014).

[36] S. Chandrasekhar and P. C. Kendall, Astrophys. J. **126**, 457 (1957).

[37] M. N. Rosenbluth and M. N. Bussak, Nucl. Fusion **19**, 489 (1979).

[38] J. Cantarella, D. DeTurck, H. Gluck, and M. Teyteld, Phys. Plasmas **7**, 2766 (2000).

[39] H.-T. Ding, A. Francis, O. Kaczmarek, F. Karsch, E. Laermann, and W. Soeldner, Phys. Rev. D **83**, 034504 (2011).

[40] G. Aarts, C. Allton, J. Foley, S. Hands, and S. Kim, Phys. Rev. Lett. **99**, 022002 (2007).

[41] A. Amato, G. Aarts, C. Allton, P. Giudice, S. Hands, and J.-I. Skullerud, arXiv:1310.7466 [hep-lat].

[42] W. Cassing, O. Linnyk, T. Steinert, and V. Ozvenchuk, Phys. Rev. Lett. **110**, 182301 (2013).

[43] K. Tuchin, J. Phys. G **39**, 025010 (2012).

[44] R. K. Mohapatra, P. S. Saumia, and A. M. Srivastava, arXiv:1102.3819 [hep-ph].